

Magnetic and magnetocaloric effect in a stuffed honeycomb antiferromagnet GdInO₃ polycrystalline

Yao-Dong Wu(吴耀东)^{a,b,c}, Wei-Wei Duan(段薇薇)^a, Qiu-Yue Li(李秋月)^a, Wei Geng(耿玮)^a, Chao Zhang(章潮)^a, Qi-Qi Lv(吕琦琦)^a, Long He(何龙)^a, Jun-Quan Chen(陈俊权)^a, Xin-Yue Hu(胡心悦)^a, Yong-Liang Qin(秦永亮)^b, Ying Meng(孟影)^a, Yuan Ma(马元)^a, Xiao-Hang Ma(马小航)^a, Zhen-Fa Zi(訾振发)^{a,*}, Jin Tang(汤进)^{b,*}

^a *Universities Joint Key Laboratory of Photoelectric Detection Science and Technology in Anhui Province, Anhui Province Key Laboratory of simulation and design for Electronic information system, and School of Physics and Materials Engineering, Hefei Normal University, Hefei, 230601, China*

^b *Anhui Province Key Laboratory of Condensed Matter Physics at Extreme Conditions, High Magnetic Field Laboratory, HFIPS, Anhui, Chinese Academy of Sciences, Hefei, 230031, China*

^c *University of Science and Technology of China, Hefei, 230026, China*

* Corresponding Author.

E-mail Address: zfzi@issp.ac.cn (Z. F. Zi); tangjin@hmfl.ac.cn (J. T.)

Keywords: GdInO₃, reversible magnetocaloric effect, magnetic refrigeration, magnetic honeycomb antiferromagnet

Abstract.

The magnetic and magnetocaloric (MCE) properties were studied in a stuffed honeycomb antiferromagnet GdInO₃ polycrystalline. No long-range magnetic ordering was observed with only a sharp upturn in the temperature dependent magnetization curves at $T_N \sim 2.1$ K. The large value of frustration index value $|\theta_w|/T_N \sim 5.0$ suggests short-range antiferromagnetic interactions existing between the Gd³⁺ moments in this frustrated magnetic system. Negligible thermal and magnetic hysteresis suggest a second-order feature of phase transition and a reversible

magnetocaloric effect (MCE) in GdInO_3 compound. In the magnetic field changes of 0–50 kOe and 0–70 kOe, the maximum magnetic entropy change values are 9.31 J/kg K and 17.53 J/kg K near the liquid helium temperature, with the corresponding *RCP* values of 106.61 and 196.38 J/kg, respectively. The relative lower MCE performance of GdInO_3 polycrystalline than the other Gd-based magnetocaloric effect is understood by the high magnetic frustration in this system. Our investigation results reveal GdInO_3 polycrystalline has a large reversible MCE, which not only provides another possibility of exploiting magnetocaloric refrigerants in the frustrated magnetic systems near the cryogenic temperature region, but also serves to excavate more exotic properties in the frustrated stuffed honeycomb magnetic systems.

Introduction

Confronting with the increasingly severe issues in terms of global warming and energy crisis, magnetic refrigeration (MR) technique based on magnetocaloric effect (MCE) of magnetic materials reveals superior advantages such as higher energy efficiency, more concentrated design as well as more environmental friendliness compared to the conventional gas-compression refrigerant ways using ozone consuming volatile refrigerants [1-3]. The searching for high-performing magnetocaloric materials has significant meanings in the future applications of MR technique near room temperature for domestic and industrial purposes [4, 5] and cryogenic temperature for hydrogen or helium liquefactions as well as space science research [6]. Recent studies demonstrated that the Gd-based compounds usually exhibited paramagnetic to long-range antiferromagnetic (AFM) magnetic transitions at the cryogenic temperature where the Gd^{3+} moments order antiferromagnetically and displayed giant MCE performances owing to the large angular momentum of half-filled $4f$ shell ($4f^7$) and negligible crystal electrical field (CEF) effect with $J = S = \frac{7}{2}, L = 0$, with representative compounds of $GdFeO_3$ [7], $GdScO_3$ [8], $GdCrO_3$ [9], $GdAlO_3$ [10], etc.

In contrast with conventional magnetic systems with long-range ferromagnetic (FM) or AFM ordering, the geometrically frustrated magnets possess peculiar lattice structures which can lead to a competition between the neighboring spin-spin interactions. Exotic magnetic properties such as spin ice and spin liquid state can be expected in geometrically frustrated magnets with Kagome, garnet, and pyrochlore lattices [11]. As a result, disordered cooperative paramagnetic ground states can remain even at temperatures much lower than the paramagnetic Curie-Weiss temperature θ_w . Up to now, many geometrically frustrated magnets have been reported to possess considerable magnetocaloric performances at cryogenic temperature region, as the quasi-paramagnetic ground states in these systems contribute no reduced entropy which can hinder the temperature change at the

adiabatic demagnetization process [11]. The typical cases are antiferromagnet $R_2M_2O_7$ ($M = \text{Ti, Mo}$) with pyrochlore lattices [12-15], the $\text{Gd}_3\text{Ga}_5\text{O}_{12}$ with garnet lattice [16], $R_3\text{BWO}_9$ with distorted Kagome magnetic lattice [17, 18], SrGd_2O_4 with distorted honeycomb magnetic lattices[19], as well as TmMgGaO_4 [20], $R\text{BO}_3$ [21], and $\text{Ba}_3\text{Ln}(\text{BO}_3)_3$ ($\text{Ln} = \text{Ho-Lu}$) with two-dimensional (2D) triangular magnetic lattices [22].

Rare-earth indium oxides $R\text{InO}_3$ possess three main types of crystal structures [23]. As the radius of rare earth ions decreases, the crystal structures can be orthorhombic with space group $Pnma$ (for $R = \text{La, Pr, Nd}$ and Sm), hexagonal with space group $P6_3cm$ (for $R = \text{Sm-Ho, Y}$), and cubic with space group $Ia\bar{3}$ (for $R = \text{Ho, Er, Yb}$). Among them, the hexagonal $R\text{InO}_3$ display fascinating properties, such as the pressure induced hexagonal to orthorhombic crystal structure transformation [24], the geometric multiferroic behavior [25], negative thermal expansion [26], etc. Particularly, the crystal structure of hexagonal $R\text{InO}_3$ consists of 2D triangular layers of R^{3+} ions separated by non-magnetic layers of corner-sharing $[\text{InO}_5]$ trigonal bipyramids [27], as shown in Fig. 1(a). Such a special magnetic lattice, which is also called the stuffed honeycomb lattice, is formed by two nonequivalent rare-earth sites R^{3+} sites with the $R1$ ions in the honeycomb sites and $R2$ at the center of each hexagon (see Fig.1(b)) [28]. If anisotropic antiferromagnetic interactions caused by spin-orbit coupling exist between the two R^{3+} sites, which is also known as the bond-dependent Kitaev interactions, a frustrated spin liquid ground state without long range magnetic ordering can be expected in the honeycomb magnetic system [29, 30]. As one important member of hexagonal $R\text{InO}_3$, TbInO_3 was recently revealed to be a highly frustrated spin liquid magnetic system with stuffed Tb^{3+} ion-based honeycomb lattice [29, 31], which is very extraordinary as the previous studies of spin-1/2 honeycomb magnets focused mostly on the $4d$ and $5d$ transition metal systems such as $\alpha\text{-RuCl}_3$ [32, 33], and the A_2IrO_3 iridates [34, 35]. Similarly, it is reported that GdInO_3 possesses no long-range magnetic ordering with only a sharp upturn below the temperature 1.8 K, indicating a magnetic frustrated ground state [26, 36]. However,

more thorough studies with various experimental and theoretical methods are requested to be done to uncover the magnetic structure at the ground state.

In this article, the magnetic and magnetocaloric effect are studied in GdInO_3 polycrystalline. The magnetic measurement results demonstrated a paramagnetic state sustained in GdInO_3 polycrystalline from room temperature to the point as low as $T_N \sim 2.1$ K, below which point a sharp increase was observed without further antiferromagnetic-like drop. In the magnetic field changes of 0–50 kOe and 0–70 kOe, the maximum magnetic entropy change values are 9.31 J/kg K and 17.53 J/kg K near the liquid helium temperature, with the corresponding RCP values of 106.61 and 196.38 J/kg, respectively. The large reversible MCE of GdInO_3 polycrystalline not only helps to understand the exotic magnetic properties of frustrated magnetic ground state in stuffed honeycomb antiferromagnet GdInO_3 , but also provides another window of the magnetocaloric refrigerants exploitation in the frustrated magnetic systems near the cryogenic temperature region.

Experiments

The GdInO_3 powders were synthesized by the conventional solid-state reaction method. High purity Gd_2O_3 (99.99 %, General Research Institute for Nonferrous Metals) and In_2O_3 (99.99 %, GRINM) powders were thoroughly mixed with equimolar amount and heated at 1673 K for 72 hours with several intermediate grindings. The phase purity and crystal structure of sample were carefully checked by a Rigaku Miniflex 624 X-ray diffractometer with high-intensity graphite monochromatized $\text{Cu-K}\alpha$ radiation at room temperature. The Rietveld refinement of XRD pattern was carried out using the Rietica software. The temperature and magnetic field dependences of magnetizations were measured on powders of ~ 2.6 mg by a Quantum Design superconducting quantum interference device vibrating sample magnetometer (SQUID-VSM) within the temperature range of 1.8–300 K.

Results and Discussion

To confirm the phase purity of the synthesized powder, the X-ray diffraction (XRD) measurement was carried out. Fig. 2(c) displays the room-temperature powder XRD pattern of the synthesized sample under Rietveld refinement. The sample exhibits a hexagonal structure with a $P6_3cm$ (No. 185) space group with refinement factors $R_p = 4.728$ and $R_{wp} = 6.267$, and no impurity was detected. All the diffraction peaks in the XRD pattern coincide with the spectral lines of the $GdInO_3$ standard card (No. 14-0150) in the Joint Committee on Powder Diffraction Standards (JCPDS) database, as shown in Fig. 2(d). The refined lattice parameters $a = 6.3569 \text{ \AA}$ and $c = 12.3512 \text{ \AA}$ agree well with the previous reported values [36].

Fig. 2 revealed the temperature dependence of magnetizations (the left vertical coordinates) under three circumstances: the ZFC and FC curves represent the data recorded upon warming up after zero-field cooled (ZFC) and field cooled (FC) from room temperature respectively, while the FCC curve denotes the data upon cooling down from room temperature under a magnetic field of 0.1 kOe. No splitting was observed between the FC and FCC curves within all the measured temperature range 1.8–300 K, indicating a negligible thermal hysteresis in this material. It is noteworthy that the paramagnetic state is kept from the room temperature down to the temperature as low as 3 K, which can be confirmed by the almost linear temperature-dependent inverse magnetization curve and the Curie-Weiss fitting in this temperature range in the right vertical coordinates of Fig. 2. The deduced effective magnetic moments $\mu_{eff} = 9.32 \mu_B / Gd$ is larger than the theoretical free Gd^{3+} ion effective moment ($\mu_{theo} = g_J \sqrt{J(J+1)} \mu_B = 7.94 \mu_B$ with $g_J = 2$, $J = S = \frac{7}{2}$), which may result from the magnetic frustrations of Gd^{3+} moments in such magnetic system. The extrapolated Curie-Weiss temperature $\theta_w = -10.50$ K indicates an antiferromagnetic feature of magnetic Gd^{3+} moments correlations. However, there is only a sharp increase in $M(T)$

curve as the first derivative value of $1/M$ becomes a peak at $T_N \sim 2.1$ K, and no more typical decrease result from the antiferromagnetic ordering is observed below this temperature point. The ratio of $|\theta_w|/T_N$ is calculated to be 5.0, revealing a moderate magnetic frustration in this magnetic system.

The magnetic field dependent magnetization hysteresis loops ($M-H$) and $\partial M/\partial H$ curves at 1.8 K and 10 K are shown in Fig. 3. No hysteresis is detected, indicating a reversible magnetocaloric effect. With the magnetic field increases, the growth rate of magnetizations at 1.8 K undergoes the first decline tendency in the magnetic field region 0–28 kOe, the following rising tendency in 28–46 kOe, and the second decline tendency in 46–70 kOe, respectively. Correspondingly, the anomalies are observed in $M-H$ hysteresis loop at ± 28 kOe with the magnetization value of $2.081 \mu_B/f.u.$ (~ 0.26 times of μ_{theo} value of free Gd^{3+} moment), which can be understood as the $M_s/3$ phenomenon induced by the collinear “up-up-down” arrangement of Gd^{3+} moments under the external magnetic field on the 2D triangular lattices. Similar results were also reported in other geometrically frustrated systems with 2D triangular magnetic lattices [37-40]. However, the growth rate of magnetizations at 10 K keeps the decline tendency in all the measured magnetic field range 0–70 kOe, which demonstrate the magnetic field induced transition is suppressed by the thermal fluctuation at high temperature. At 1.8 K, the magnetization value reaches $4.81 \mu_B/f.u.$ (107.47 emu/g) under 70 kOe, which corresponds to only ~ 60.5 % of the expected theoretical Gd^{3+} ion magnetic moments ($7.94 \mu_B/f.u.$). Compared to the other reported Gd^{3+} -based compounds such as $GdScO_3$ [8], $GdFeO_3$ [41] and $GdCoO_3$ [42], the field dependent magnetizations of $GdInO_3$ reveal slower growth rate and much lower values at the same magnetic fields, which can be attributed to the stuffed honeycomb lattice induced magnetic frustrations. Based on the magnetic field dependent magnetizations in the temperature region 2–50 K, as shown in Fig. 4(a), the Arrott plot of $GdInO_3$ is drawn in Fig. 4(b). All the data lines display positive slopes, which confirm a second-order character of magnetic field induced magnetic transition according to the Banerjee criterion [43].

Considering the prominent field dependent magnetizations with negligible thermal and magnetization hysteresis, an expectation of a large reversible MCE can be made in GdInO₃ polycrystalline. By using the Maxwell relation, the magnetic entropy change $-\Delta S_M$ are calculated based on the M - H data, as shown in the following equation [6]:

$$\Delta S_M(T, H) = \int_0^H \left(\frac{\partial S}{\partial H}\right)_T dH = \int_0^H \left(\frac{\partial M}{\partial T}\right)_H dH = \sum_0^H \left(\frac{M_{T_1} - M_{T_2}}{T_1 - T_2}\right) \Delta H, \quad (1)$$

where M_{T_1} and M_{T_2} represent the magnetizations at temperatures T_1 and T_2 respectively for a magnetic field change of ΔH . Fig. 5(a) denotes the temperature dependence of the magnetic entropy changes of GdInO₃ under the magnetic fields 1–70 kOe. Owing to the quite low value of Gd³⁺ ordering temperature ($T_N \sim 2.1$ K), the maximums of the magnetic entropy changes lie in the temperature below 5 K within all the measured magnetic field region, and only the hot half parts of $-\Delta S_M$ peaks are observed within the temperature range 3–49 K. In the magnetic field changes of 0–20 kOe, 0–50 kOe, 0–70 kOe, the maximum magnetic entropy values are 2.89 J/kg K, 9.31 J/kg K and 17.53 J/kg K, respectively. Additionally, the other two crucial parameters to estimate the MCE performance are the refrigerant capacity (RC) and the relative cooling power (RCP). For convenience, they are called R factors in this paper and are defined as follows [44]:

$$RC = -\int_{T_1}^{T_2} \Delta S_M(T) dT, \quad (2)$$

$$RCP = -\Delta S_M^{\max} \times \delta T_{FWHM} \quad (3)$$

where $-\Delta S_M^{\max}$, T_1 , T_2 and δT_{FWHM} represent the maximum value of $-\Delta S_M$, the cold end, the hot end and the interval of temperature that mark the half maximum $-\Delta S_M$, respectively. Considering the the cold temperature ends of half $-\Delta S_M^{\max}$ values are below the lowest measurement limit (1.8 K), we simply adopt 3 K as T_1 and obtain the R factors under different magnetic field in the inset of Fig. 5(b). In the field changes of 0–50 and 0–70 kOe, the RC values are 82.01 and 150.67 J/kg respectively,

and the *RCP* values are 106.61 and 196.38 J/kg, respectively. The magnetocaloric effect of GdInO₃ demonstrate a much lower value than the other Gd-based compounds, such as GdScO₃, GdCrO₃, GdAlO₃, etc [8-10, 41, 42], which may result from the stuffed honeycomb lattice induced magnetic frustrations between Gd³⁺ moments. However, the maximum magnetic entropy change $-\Delta S_M^{\max}$ (17.53 J/kg K) and the *R* factors (150.67 J/kg fo *RC*, 196.38 J/kg for *RCP*) under the magnetic field change 0–70 kOe still show a comparable or even larger values than some rare earth based compounds near the liquid helium temperature such as *R*FeO₃ (*R* = Dy, Tm) [45, 46], *R*₂Mo₂O₇ (*R* = Gd, Er, Dy) [15], DyVWO₆ [47], *R*₂CrMnO₆ (*R* = Ho and Er) [48], *R*₂FeCrO₆ (*R* = Er and Tm) [49], Li*Ln*P₄O₁₂ (*Ln* = Tb, Dy) [50], *R*VO₄ (*R* = Er, Ho and Yb) [51], *RAgAl* (*R* = Er, Ho)[52]. The experimental results in our work indicate GdInO₃ owns a large reversible MCE near the liquid helium temperature, which not only helps to explore the complicated mechanisms in the frustrated stuffed honeycomb magnetic lattices, but also offers great potential for the applications of frustrated magnetic systems in the future low-temperature magnetic refrigeration.

Conclusions

In summary, we performed the magnetic and magnetocaloric investigations on polycrystalline GdInO_3 . The magnetic measurements on GdInO_3 show the paramagnetic state is kept from room temperature to the Néel temperature $T_N \sim 2.1$ K. The large value of $|\theta_w|/T_N$ and the magnetization value of only 60.5 % percent of free Gd^{3+} moments at 1.8 K and 70 kOe all reveal a frustration existing in this stuffed honeycomb antiferromagnet system. No thermal and magnetization hysteresis are observed, which indicate a reversible MCE performance. In the magnetic field changes of 0–50 and 0–70 kOe, the maximum magnetic entropy changes of 9.31 J/kg K and 17.53 J/kg K are obtained near the liquid helium temperature. Correspondingly, the RC values are 82.01 and 150.67 J/kg respectively, and the RCP values are 106.61 and 196.38 J/kg, respectively. The relatively lower MCE performance of GdInO_3 than the other Gd-based compounds may be the result of the triangular-honeycomb magnetic Gd^{3+} lattice caused magnetic frustration. However, the comparable MCE with the other typical magnetocaloric materials, as well as the reversible feature all suggest that the GdInO_3 display superior potential in the future application of magnetic refrigeration near the liquid helium temperature.

Acknowledgments

This work was supported by the National Natural Sciences Foundation of China (Grant No. 12104123, U1632161), Anhui Provincial Funds for Distinguished Young Scientists of the Nature Science (Grant No. 1808085JQ13), the Natural Science Foundation of Anhui Province (Grant No. 2008085MF217), Universities Joint Key Laboratory of Photoelectric Detection Science and Technology in Anhui Province (Grant No. 2019GDTC06), the open fund project from Anhui Province Key Laboratory of simulation and design for Electronic information system (Grant No. 2019ZDSYSZY04), the Project of Leading Backbone Talents in Anhui Provincial Undergraduate Universities, and Undergraduate Innovation and Entrepreneurship Training Program in Anhui Province (Grant No. S202014098164).

Figure captions

Fig. 1. (a) The hexagonal $P6_3cm$ crystal structure of $GdInO_3$. (b) The stuffed honeycomb arrangement of Gd1 and Gd2 sites in the ab plane. The green, blue, white, and red balls denote Gd1, Gd2, In and O atoms respectively. The colored thick solid sticks represent the atomic bonds. The black solid lines constitute the crystal unit cells of $GdInO_3$. (c) XRD pattern of $GdInO_3$ polycrystalline measured at room temperature. The cross-shaped symbols and red solid line represent the experimental data and Rietveld refined results respectively. The blue line is the difference between the experiment and fitting results. (d) Standard card (No. 14-0150) of powdered $GdInO_3$ in the Joint Committee on Powder Diffraction Standards (JCPDS) database.

Fig. 2. Temperature dependences of ZFC, FCC and FC magnetizations (the left vertical coordinates) and ZFC inverse magnetizations fitted by the Curie-Weiss law (the right vertical coordinates) of $GdInO_3$ polycrystalline under a field of 0.1 kOe. The inset displays the temperature dependence of the first derivative values of ZFC magnetizations (blue triangle symbols) of $GdInO_3$ polycrystalline under a field of 0.1 kOe.

Fig. 3. (a) The magnetization hysteresis (M - H) loops measured at 1.8 (blue line) and 10 K (red line) respectively of $GdInO_3$ polycrystalline under a magnetic field range from -70 kOe to $+70$ kOe. (b) The first derivative curves of magnetic field dependent M - H loops at 1.8 (blue square symbols) and 10 K (red circle symbols) respectively.

Fig. 4. (a) Magnetic field dependence of isothermal magnetizations in the temperature range of 2–50 K with an interval of 2 K. (b) Arrott plot of $GdInO_3$ polycrystalline in the temperature range of 2–50 K.

Fig. 5. (a) Temperature dependence of magnetic entropy changes $-\Delta S_M^R$ of $GdInO_3$ polycrystalline. (b) The magnetic field dependences of RC (magenta hexagon symbols) and RCP (blue star symbols) curves.

Reference:

- [1] V.K. Pecharsky, K.A. Gschneidner Jr, Magnetocaloric effect and magnetic refrigeration, *J. Magn. Magn. Mater.* , 200 (1999) 44-56.
- [2] Y.-H. Ding, F.-Z. Meng, L.-C. Wang, R.-S. Liu, J. Shen, Metamagnetic transition and reversible magnetocaloric effect in antiferromagnetic DyNiGa compound, *Chin. Phys. B.* , 29 (2020) 077501.
- [3] J.-Z. Hao, F.-X. Hu, Z.-B. Yu, F.-R. Shen, H.-B. Zhou, Y.-H. Gao, K.-M. Qiao, J. Li, C. Zhang, W.-H. Liang, J. Wang, J. He, J.-R. Sun, B.-G. Shen, Multicaloric and coupled-caloric effects, *Chin. Phys. B.* , 29 (2020) 047504.
- [4] V. Franco, J.S. Blázquez, B. Ingale, A. Conde, The Magnetocaloric Effect and Magnetic Refrigeration Near Room Temperature: Materials and Models, *Annual Review of Materials Research*, 42 (2012) 305-342.
- [5] M.A.A. Bally, M.A. Islam, S.M. Hoque, R. Rashid, M. Fakhru Islam, F.A. Khan, Magnetocaloric properties and analysis of the critical point exponents of $\text{Pr}_{0.55}\text{Ca}_x\text{Sr}_{0.45-x}\text{MnO}_3$ ($x = 0.00, 0.05, 0.1$ and 0.2) at PM-FM phase transition, *Results in Physics*, 28 (2021) 104546.
- [6] B.G. Shen, J.R. Sun, F.X. Hu, H.W. Zhang, Z.H. Cheng, Recent Progress in Exploring Magnetocaloric Materials, *Adv. Mater.* , 21 (2009) 4545-4564.
- [7] M. Das, S. Roy, P. Mandal, Giant reversible magnetocaloric effect in a multiferroic GdFeO_3 single crystal, *Phys. Rev. B*, 96 (2017) 174405.
- [8] Y.-D. Wu, H. Chen, J.-Y. Hua, Y.-L. Qin, X.-H. Ma, Y.-Y. Wei, Z.-F. Zi, Giant reversible magnetocaloric effect in orthorhombic GdScO_3 , *Ceram. Int.* , 45 (2019) 13094-13098.
- [9] S. Mahana, U. Manju, D. Topwal, GdCrO_3 : a potential candidate for low temperature magnetic refrigeration, *J. Phys. D: Appl. Phys.* , 51 (2018) 305002.
- [10] S. Mahana, U. Manju, D. Topwal, Giant magnetocaloric effect in GdAlO_3 and a comparative study with GdMnO_3 , *J. Phys. D: Appl. Phys.* , 50 (2017) 035002.
- [11] M.E. Zhitomirsky, Enhanced magnetocaloric effect in frustrated magnets, *Phys. Rev. B*, 67 (2003) 104421.
- [12] S.S. Sosin, L.A. Prozorova, A.I. Smirnov, A.I. Golov, I.B. Berkutov, O.A. Petrenko, G. Balakrishnan, M.E. Zhitomirsky, Magnetocaloric effect in pyrochlore antiferromagnet $\text{Gd}_2\text{Ti}_2\text{O}_7$, *Phys. Rev. B*, 71 (2005) 094413.
- [13] M. Orendáč, J. Hanko, E. Čížmár, A. Orendáčová, M. Shirai, S.T. Bramwell, Magnetocaloric study of spin relaxation in dipolar spin ice $\text{Dy}_2\text{Ti}_2\text{O}_7$, *Phys. Rev. B*, 75 (2007) 104425.
- [14] H. Aoki, T. Sakakibara, K. Matsuhira, Z. Hiroi, Magnetocaloric Effect Study on the Pyrochlore Spin Ice Compound $\text{Dy}_2\text{Ti}_2\text{O}_7$ in a [111] Magnetic Field, *J. Phys. Soc. Jpn.* , 73 (2004) 2851-2856.
- [15] Y.-D. Wu, Q.-Y. Dong, Y. Ma, Y.-J. Ke, N. Su, X.-Q. Zhang, L.-C. Wang, Z.-H. Cheng, Phase transition-induced magnetocaloric effects in $R_2\text{Mo}_2\text{O}_7$ ($R = \text{Er}, \text{Dy}, \text{Gd}$ and Y) molybdates, *Mater. Lett.* , 198 (2017) 110-113.
- [16] N.K. Chogondahalli Muniraju, R. Baral, Y. Tian, R. Li, N. Poudel, K. Gofryk, N. Barisic, B. Kiefer, J.H. Ross, Jr., H.S. Nair, Magnetocaloric Effect in a Frustrated Gd-Garnet with No Long-Range Magnetic Order, *Inorg. Chem.* , 59 (2020) 15144-15153.
- [17] L.-L. Li, X.-Y. Yue, W.-J. Zhang, H. Bao, D.-D. Wu, H. Liang, Y.-Y. Wang, Y. Sun, Q.-J. Li, X.-F. Sun, Magnetism and giant magnetocaloric effect in rare-earth-based compounds $R_3\text{BWO}_9$ ($R = \text{Gd}, \text{Dy}, \text{Ho}$), *Chin. Phys. B.* , 30 (2021) 077501.
- [18] Z. Yang, H. Zhang, M. Bai, W. Li, S. Huang, S. Ruan, Y.-J. Zeng, Large magnetocaloric effect in

- gadolinium borotungstate Gd_3BWO_9 , Journal of Materials Chemistry C, 8 (2020) 11866-11873.
- [19] X. Jiang, Z.W. Ouyang, Z.X. Wang, Z.C. Xia, G.H. Rao, Magnetization, ESR and large magnetocaloric effect in zigzag chain $SrGd_2O_4$, J. Phys. D: Appl. Phys. , 51 (2018) 045001.
- [20] Y. Li, S. Bachus, H. Deng, W. Schmidt, H. Thoma, V. Hutanu, Y. Tokiwa, A.A. Tsirlin, P. Gegenwart, Partial Up-Up-Down Order with the Continuously Distributed Order Parameter in the Triangular Antiferromagnet $TmMgGaO_4$, Physical Review X, 10 (2020) 011007.
- [21] P. Mukherjee, Y. Wu, G.I. Lampronti, S.E. Dutton, Magnetic properties of monoclinic lanthanide orthoborates, $LnBO_3$, $Ln = Gd, Tb, Dy, Ho, Er, Yb$, Mater. Res. Bull. , 98 (2018) 173-179.
- [22] N.D. Kelly, C. Liu, S.E. Dutton, Structure and magnetism of a new hexagonal polymorph of $Ba_3Tb(BO_3)_3$ with a quasi-2D triangular lattice, J. Solid State Chem. , 292 (2020) 121640.
- [23] R. Kaiwart, A. Dwivedi, R. Shukla, S. Velaga, V. Grover, H.K. Poswal, High pressure structural evolution of cubic solid solution $YbInO_3$, J. Appl. Phys. , 130 (2021) 035902.
- [24] C. Lin, J. Liu, Y. Li, X. Li, R. Li, Pressure-induced structural and vibrational evolution in ferroelectric $RInO_3$ ($R=Eu, Gd, Dy$), Solid State Commun. , 173 (2013) 51-55.
- [25] T. Tohei, H. Moriwake, H. Murata, A. Kuwabara, R. Hashimoto, T. Yamamoto, I. Tanaka, Geometric ferroelectricity in rare-earth compounds $RGaO_3$ and $RInO_3$, Phys. Rev. B, 79 (2009) 144125.
- [26] B. Paul, S. Chatterjee, A. Roy, A. Midya, P. Mandal, V. Grover, A.K. Tyagi, Geometrically frustrated $GdInO_3$: An exotic system to study negative thermal expansion and spin-lattice coupling, Phys. Rev. B, 95 (2017) 054103.
- [27] E.E. Gordon, X. Cheng, J. Kim, S.W. Cheong, S. Deng, M.H. Whangbo, Nonequivalent Spin Exchanges of the Hexagonal Spin Lattice Affecting the Low-Temperature Magnetic Properties of $RInO_3$ ($R = Gd, Tb, Dy$): Importance of Spin-Orbit Coupling for Spin Exchanges between Rare-Earth Cations with Nonzero Orbital Moments, Inorg. Chem. , 57 (2018) 9260-9265.
- [28] J. Sahoo, R. Flint, Symmetric spin liquids on the stuffed honeycomb lattice, Phys. Rev. B, 101 (2020).
- [29] L. Clark, G. Sala, D.D. Maharaj, M.B. Stone, K.S. Knight, M.T.F. Telling, X. Wang, X. Xu, J. Kim, Y. Li, S.-W. Cheong, B.D. Gaulin, Two-dimensional spin liquid behaviour in the triangular-honeycomb antiferromagnet $TbInO_3$, Nat. Phys. , 15 (2019) 262-268.
- [30] L. Janssen, E.C. Andrade, M. Vojta, Honeycomb-Lattice Heisenberg-Kitaev Model in a Magnetic Field: Spin Canting, Metamagnetism, and Vortex Crystals, Phys. Rev. Lett. , 117 (2016) 277202.
- [31] J. Kim, X. Wang, F.-T. Huang, Y. Wang, X. Fang, X. Luo, Y. Li, M. Wu, S. Mori, D. Kwok, E.D. Mun, V.S. Zapf, S.-W. Cheong, Spin Liquid State and Topological Structural Defects in Hexagonal $TbInO_3$, Physical Review X, 9 (2019) 031005.
- [32] A. Banerjee, J. Yan, J. Knolle, C.A. Bridges, M.B. Stone, M.D. Lumsden, D.G. Mandrus, D.A. Tennant, R. Moessner, S.E. Nagler, Neutron scattering in the proximate quantum spin liquid α - $RuCl_3$, Science, 356 (2017) 1055.
- [33] S.-H. Do, S.-Y. Park, J. Yoshitake, J. Nasu, Y. Motome, Yong S. Kwon, D.T. Adroja, D.J. Voneshen, K. Kim, T.H. Jang, J.H. Park, K.-Y. Choi, S. Ji, Majorana fermions in the Kitaev quantum spin system α - $RuCl_3$, Nat. Phys. , 13 (2017) 1079-1084.
- [34] Y. Singh, S. Manni, J. Reuther, T. Berlijn, R. Thomale, W. Ku, S. Trebst, P. Gegenwart, Relevance of the Heisenberg-Kitaev model for the honeycomb lattice iridates A_2IrO_3 , Phys. Rev. Lett. , 108 (2012) 127203.
- [35] X. Liu, T. Berlijn, W.G. Yin, W. Ku, A. Tsvelik, Y.-J. Kim, H. Gretarsson, Y. Singh, P. Gegenwart, J.P. Hill, Long-range magnetic ordering in Na_2IrO_3 , Phys. Rev. B, 83 (2011) 220403.

- [36] Y. Li, Y. Wang, W. Tan, W. Wang, J. Zhang, J.W. Kim, S.-W. Cheong, X. Tao, Laser floating zone growth of improper geometric ferroelectric GdInO_3 single crystals with Z6 topological defects, *Journal of Materials Chemistry C*, 6 (2018) 7024-7029.
- [37] D.J. Farnell, R. Zinke, J. Schulenburg, J. Richter, High-order coupled cluster method study of frustrated and unfrustrated quantum magnets in external magnetic fields, *J Phys Condens Matter*, 21 (2009) 406002.
- [38] J. Alicea, A.V. Chubukov, O.A. Starykh, Quantum stabilization of the $1/3$ -magnetization plateau in Cs_2CuBr_4 , *Phys. Rev. Lett.*, 102 (2009) 137201.
- [39] T. Susuki, N. Kurita, T. Tanaka, H. Nojiri, A. Matsuo, K. Kindo, H. Tanaka, Magnetization process and collective excitations in the $S=1/2$ triangular-lattice Heisenberg antiferromagnet $\text{Ba}_3\text{CoSb}_2\text{O}_9$, *Phys. Rev. Lett.*, 110 (2013) 267201.
- [40] S. Bachus, I.A. Iakovlev, Y. Li, A. Wörl, Y. Tokiwa, L. Ling, Q. Zhang, V.V. Mazurenko, P. Gegenwart, A.A. Tsirlin, Field evolution of the spin-liquid candidate YbMgGaO_4 , *Phys. Rev. B*, 102 (2020).
- [41] Y.-J. Ke, X.-Q. Zhang, J.-F. Wang, Z.-H. Cheng, Giant magnetic entropy change in gadolinium orthoferrite near liquid hydrogen temperature, *J. Alloys Compd.*, 739 (2018) 897-900.
- [42] Q.Y. Dong, K.Y. Hou, X.Q. Zhang, L. Su, L.C. Wang, Y.J. Ke, H.T. Yan, Z.H. Cheng, Giant reversible magnetocaloric effect in antiferromagnetic rare-earth cobaltite GdCoO_3 , *J. Appl. Phys.*, 127 (2020) 033904.
- [43] A. Arrott, J.E. Noakes, Approximate Equation of State For Nickel Near its Critical Temperature, *Phys. Rev. Lett.*, 19 (1967) 786-789.
- [44] L.-W. Li, Review of magnetic properties and magnetocaloric effect in the intermetallic compounds of rare earth with low boiling point metals, *Chin. Phys. B.*, 25 (2016) 037502.
- [45] Y.-J. Ke, X.-Q. Zhang, H. Ge, Y. Ma, Z.-H. Cheng, Low field induced giant anisotropic magnetocaloric effect in DyFeO_3 single crystal, *Chin. Phys. B.*, 24 (2015) 037501.
- [46] Y.J. Ke, X.Q. Zhang, Y. Ma, Z.H. Cheng, Anisotropic magnetic entropy change in $R\text{FeO}_3$ single crystals ($R = \text{Tb}, \text{Tm}, \text{or Y}$), *Sci Rep*, 6 (2016) 19775.
- [47] P. Yanda, A. Sundaresan, Magnetism, magnetocaloric and magnetodielectric properties of DyVWO_6 : a new aeschynite-type polar antiferromagnet, *Materials Research Express*, 6 (2020) 124007.
- [48] B. Wu, D. Guo, Y. Wang, Y. Zhang, Crystal structure, magnetic properties, and magnetocaloric effect in B-site disordered $RE_2\text{CrMnO}_6$ ($RE = \text{Ho}$ and Er) perovskites, *Ceram. Int.*, 46 (2020) 11988-11993.
- [49] Z. Dong, Z. Wang, S. Yin, Structural, magnetic and cryogenic magneto-caloric properties in $RE_2\text{FeCrO}_6$ ($RE = \text{Er}$ and Tm) compounds, *Ceram. Int.*, 46 (2020) 26632-26636.
- [50] D.N. Petrov, P.T. Long, Y.S. Koshkid'ko, J. Ćwik, K. Nenkov, Large magnetocaloric effect in $\text{LiLnP}_4\text{O}_{12}$ ($Ln = \text{Gd}, \text{Tb}, \text{Dy}$) single crystals, *J. Phys. D: Appl. Phys.*, 53 (2020) 495005.
- [51] K. Dey, A. Indra, S. Majumdar, S. Giri, Cryogenic magnetocaloric effect in zircon-type $R\text{VO}_4$ ($R = \text{Gd}, \text{Ho}, \text{Er}, \text{and Yb}$), *Journal of Materials Chemistry C*, 5 (2017) 1646-1650.
- [52] Y. Zhang, B. Yang, G. Wilde, Magnetic properties and magnetocaloric effect in ternary $RE\text{AgAl}$ ($RE = \text{Er}$ and Ho) intermetallic compounds, *J. Alloys Compd.*, 619 (2015) 12-15.

Figures:

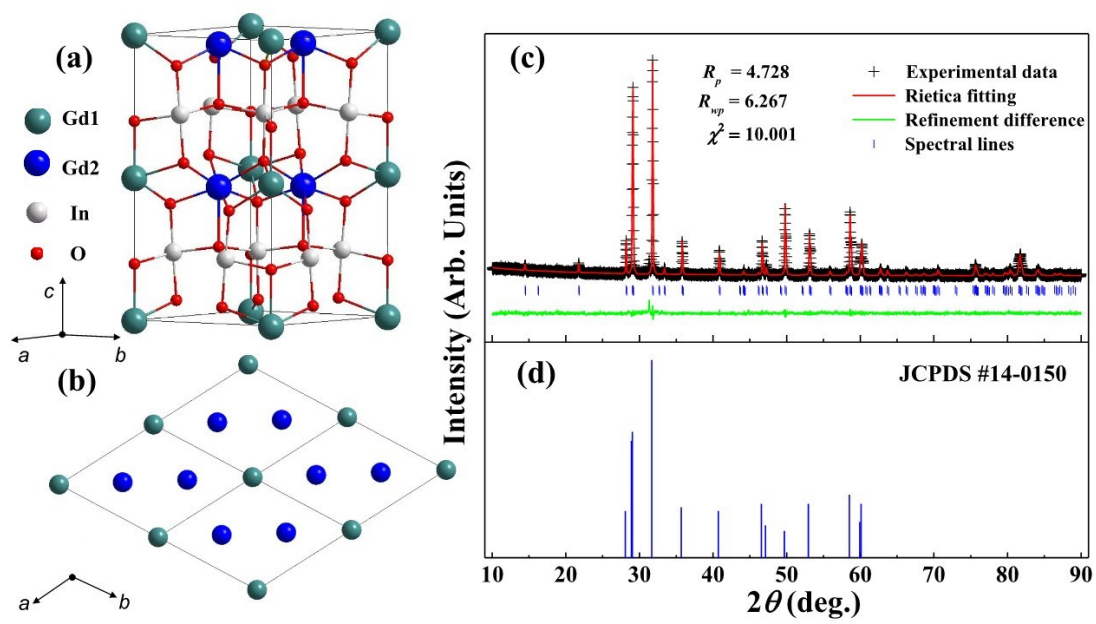


Fig. 1.

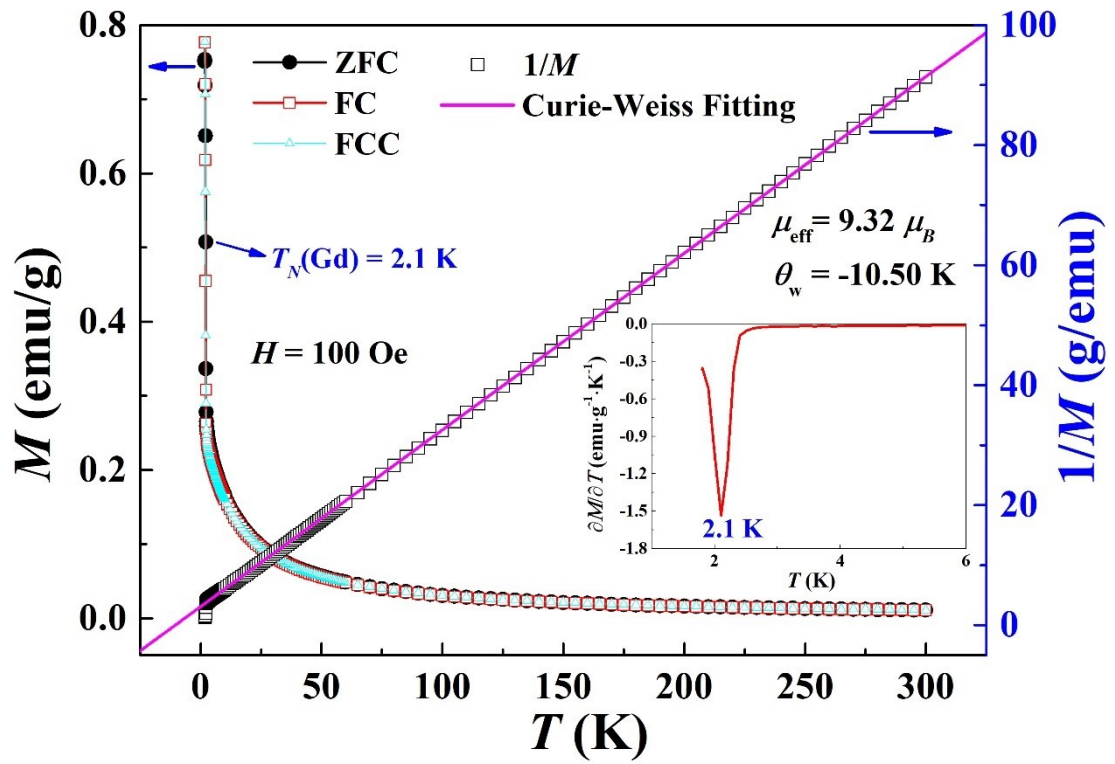


Fig. 2.

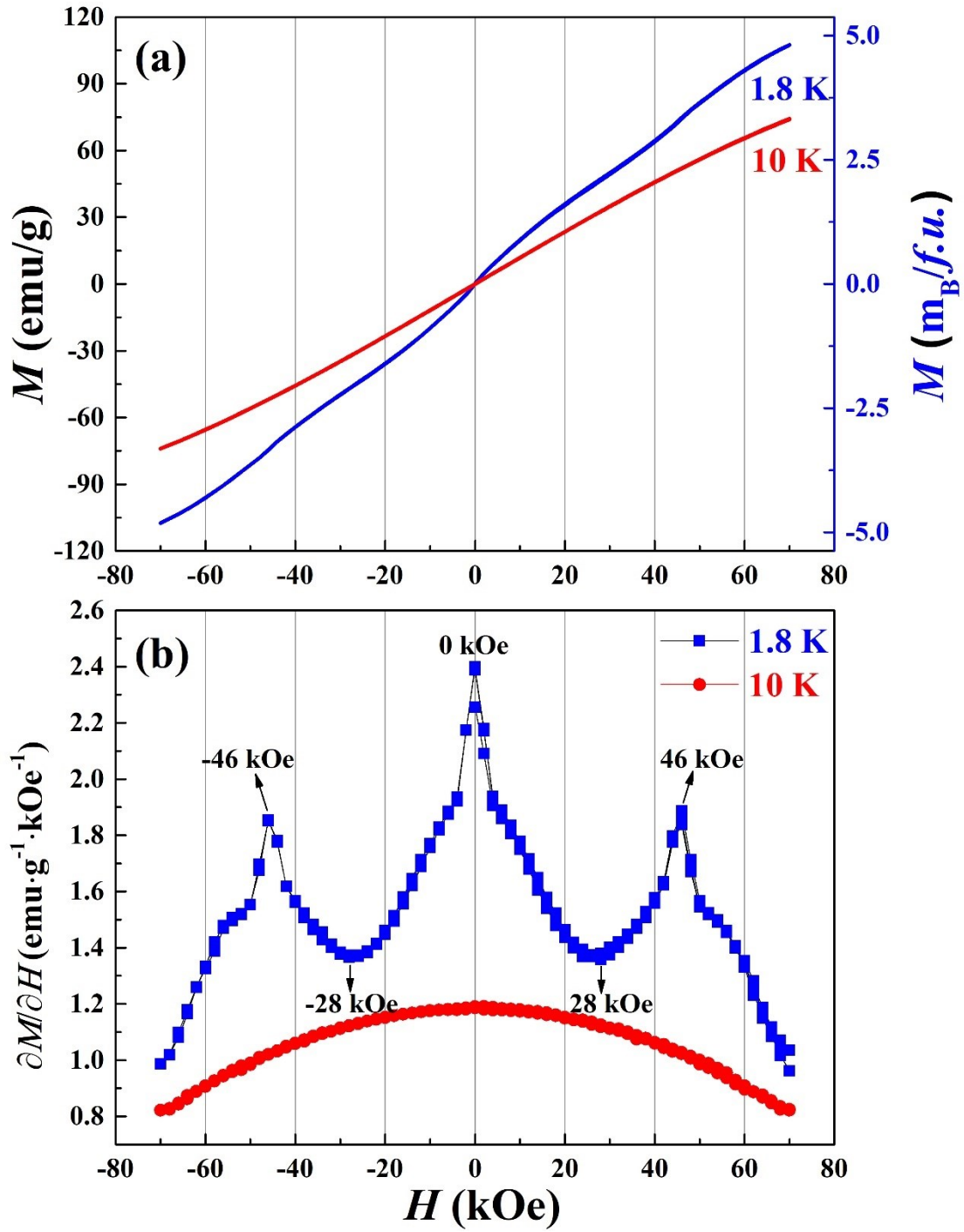


Fig. 3.

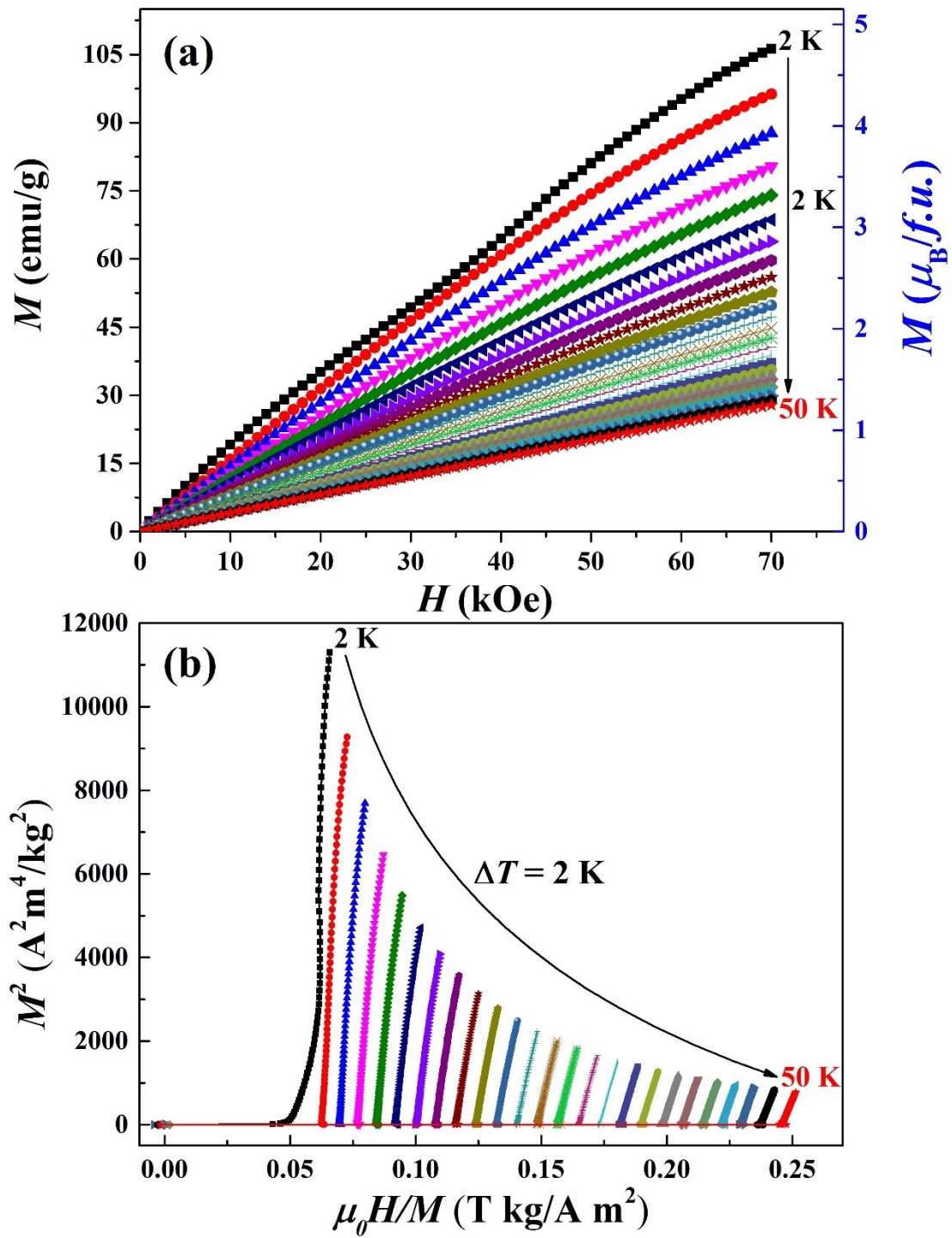


Fig. 4.

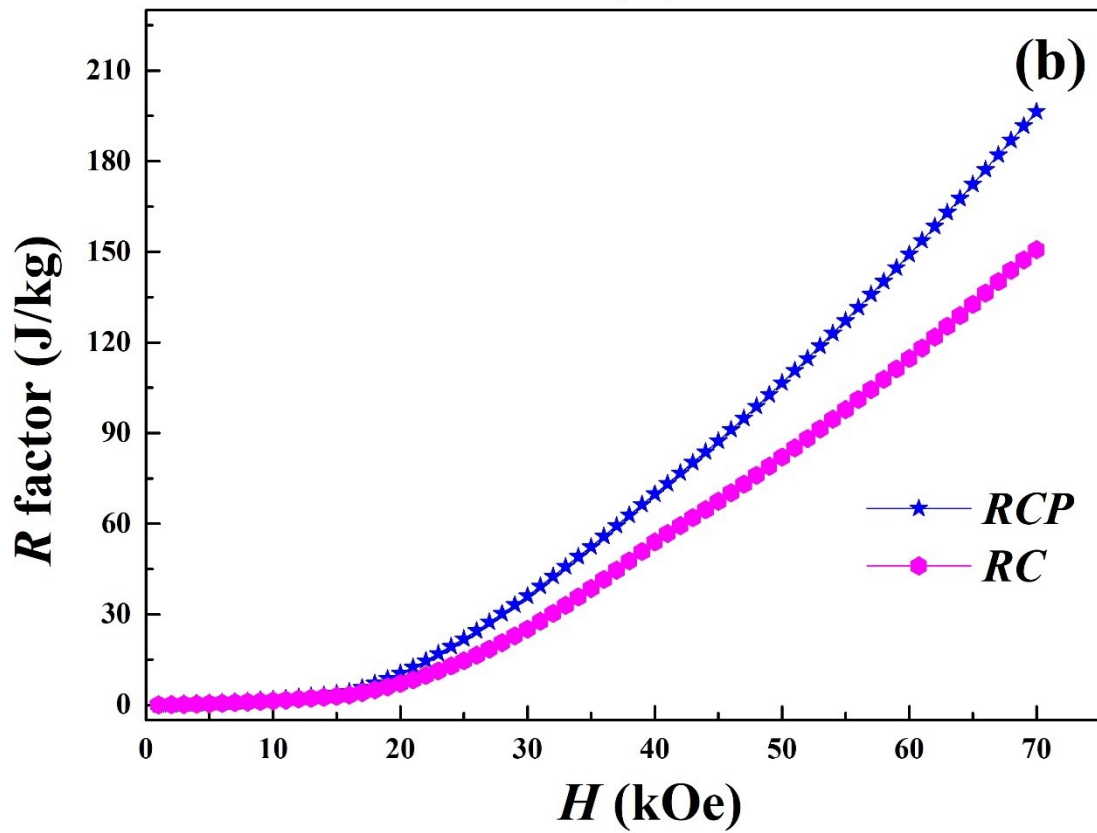
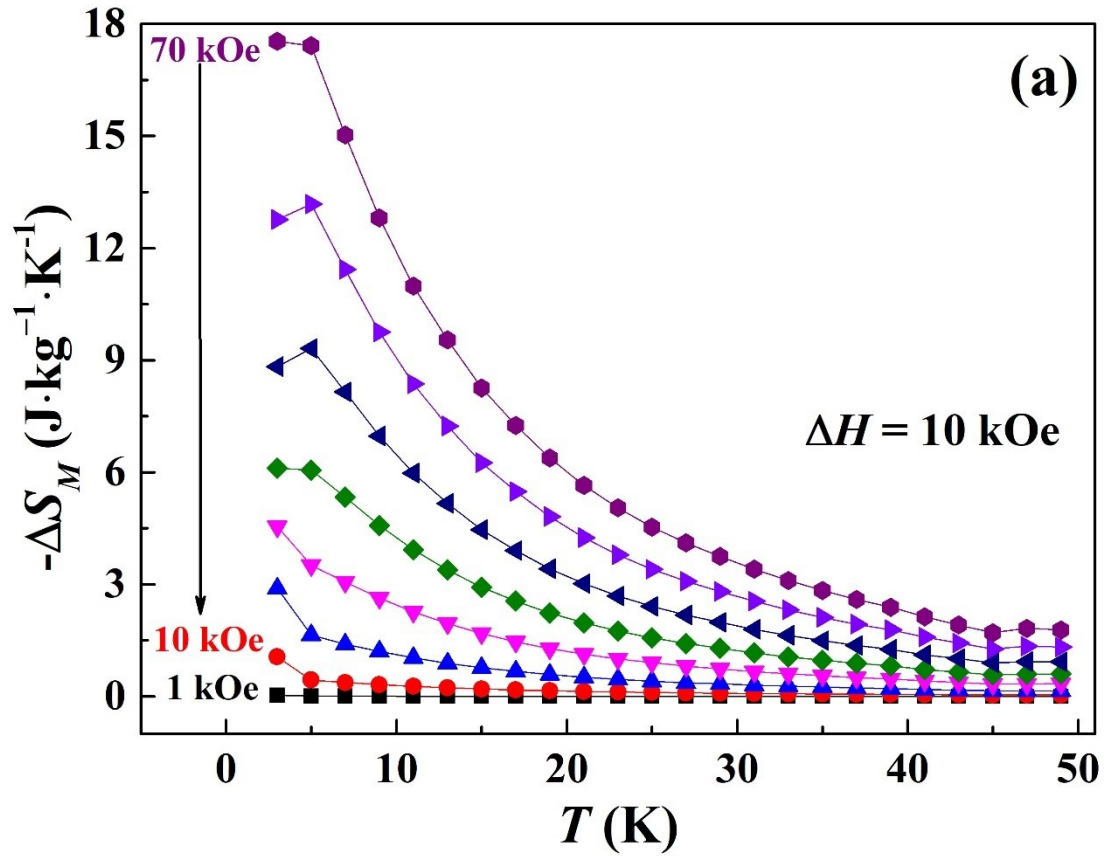


Fig. 5.